

Denoising Medical Ultrasound Images and Error Estimate by Translation-Invariant Wavelets

R. Bouchouareb, N. Hedjazi, and D. Benatia

*University of Batna, Faculty of Engineering Sciences, Department of Electronic,
Batna, ALGERIA
rachidabouchouareb@gmail.com*

Abstract

Speckle Noise is a natural characteristic of medical ultrasound images. It is a term used for the granular form that appears in B-Scan and can be considered as a kind of multiplicative noise. Speckle Noise reduces the ability of an observer to distinguish fine details in diagnostic testing. It also limits the effective implementation of image processing such as edge detection, segmentation and volume rendering in 3 D. Therefore; treatment methods of speckle noise were sought to improve the image quality and to increase the capacity of diagnostic medical ultrasound images. Such as median filters, Wiener and linear filters (Persona & Malik, SRAD). The method used in this work is 2-D translation invariant forward wavelet transform, it is used in image processing, including noise reduction applications in medical imaging.

Keywords: *wavelets transform, image processing, ultrasound image, filtering*

1. Introduction

Methods of image processing for speckle noise reduction were sought to improve the image quality and enhance the diagnostic capabilities of medical ultrasound images. The first approach to remove speckle noise is the Wiener filter developed by Jain and adaptive weighted median filter proposed by Loupas, but they fail to preserve the details useful because of the low-pass filters only. Despite the noise of the speckle is a successful process and failed. The statistical noise stains can be useful to distinguish between each type and composition of tissues.

It was also recognized that the linear filtering is far from being an appropriate method used to reduce speckle noise. Over the past decade, there has been considerable interest in using the wavelet transform as an effective method to reduce noise spots. Zong and others [1] have used a logarithmic transformation to separate the noise from the original image. Simoncelli and others [2] have developed non-linear estimators, based on formal Bayesian theory, which exceed the standard linear processors and simple thresholding estimators in reducing noise from natural images. Achime and others [3, 4] have developed a posterior estimator (CARD) for ultrasound images, assuming an alpha-stable prior to the signal. Yu made the SRAD [5] method (reducing speckle with anisotropic diffusion) based on partial differential equations. Most of these techniques assume that after a logarithmic transformation, the stain can be approximated by additive Gaussian noise of zero mean and estimators / filters are designed accordingly.

In this paper we have discussed in detail a new method that is used in image processing and its applications including noise reduction in medical imaging, this method 2-D translation invariant forward wavelet transform.

2. Wavelets

A wavelet function $\psi(t)$ is a small wave, which must be oscillatory in some way to discriminate between different frequencies. The wavelet contains both the analyzing shape and the window. Figure1 shows an example of a possible wavelet, known as the Morlet wavelet. For the CWT several kind of wavelet functions are developed which all have specific properties.

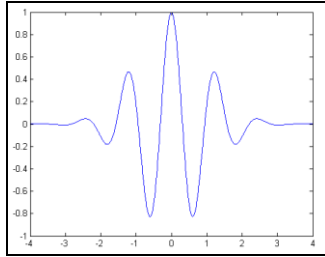


Figure 1. Morlet Wavelet

An analyzing function $\psi(t)$ is classified as a wavelet if the following mathematical criteria are satisfied:

1. A wavelet must have finite energy

$$E = \int_{-\infty}^{\infty} |\psi(t)|^2 dt < \infty$$

The energy E equals the integrated squared magnitude of the analyzing function $\psi(t)$ and must be less than infinity.

2. If $\hat{\psi}(f)$ is the Fourier transform of the wavelet $\psi(t)$, the following condition must hold

$$C_{\psi} = \int_0^{\infty} \frac{|\hat{\psi}(f)|^2}{f} df < \infty$$

This condition implies that the wavelet has no zero frequency component ($\psi(0) = 0$), i.e. the mean of the wavelet $\psi(t)$ must equal zero. This condition is known as the admissibility constant. The value of C_{ψ} depends on the chosen wavelet.

3. For complex wavelets the Fourier transform $\hat{\psi}(f)$ must be both real and vanish for negative frequencies[6].

3. Two Dimensional Dwt (2d dwt)

At the base of the 2D DWT's implementation relies the concept of separable multiresolutions and of two-dimensional wavelet bases, notions that we will define further.

Let $\{V_j\}_{j \in \mathbb{Z}}$ be a multiresolution of $L^2(\mathbb{R})$. A separable two-dimensional resolution is composed of the tensor product spaces

$$V_j^2 = V_j \otimes V_j \tag{1}$$

The space V_j^2 is a set of finite energy functions $x(t_1, t_2)$ that are linear expansions of separable functions

$$x(t_1, t_2) = \sum_{m=-\infty}^{\infty} a[m] f_m(t_1) g_m(t_2) \text{ with } f_m, g_m \in V_j \tag{2}$$

A separable wavelet orthonormal basis of $L^2(\mathbb{R}^2)$ is constructed with separable products of a scaling function ϕ and a wavelet ψ , being associated to a one-dimensional multiresolution approximation $\{V_j\}_{j \in \mathbb{Z}}$. Let W_j^2 be the detail space equal to the orthogonal complement of the lower resolution approximation space V_j^2 in V_{j-1}^2 ,

$$V_{j-1}^2 = V_j^2 \otimes W_j^2 \quad (3)$$

To construct a wavelet orthonormal basis of $L^2(\mathbb{R}^2)$, the following theorem builds a wavelet basis of each detail space W_j^2 .

Let $h[n]$ and $g[n]$ be the conjugate mirror filters associated to the wavelet ψ . We denote with $f_d[n]$ the mirror filter associated to $f[n]$, $f_d[n] = f[-n]$.

The wavelet coefficients at the scale 2^{j+1} are calculated from the approximation coefficients at scale 2^j , a_j , with two-dimensional separable convolutions and subsamplings.

The decomposition formula are obtained by applying the one-dimensional convolution formula

$$a_{j+1}[p] = \langle x, \phi_{j+1,p} \rangle = \sum_{n=-\infty}^{\infty} h[n-2p] \langle x, \phi_{j,p} \rangle = \sum_{n=-\infty}^{\infty} h[n-2p] a_j[n] = a_j[p] * h_d[2p] \quad (4)$$

And, respectively,

$$d_{j+1}[p] = \langle x, \sum_{n=-\infty}^{\infty} g[n-2p] \phi_{j,n} \rangle = \sum_{n=-\infty}^{\infty} g[n-2p] \langle x, \phi_{j,n} \rangle = \sum_{n=-\infty}^{\infty} g[n-2p] a_j[n] = a_j[p] * g_d[2p] \quad (5)$$

To the separable two-dimensional wavelets and scaling functions:

$$\begin{aligned} a_{j+1}[n_1, n_2] &= a_j[n_1, n_2] * h_d[2n_1] h_d[2n_2] \\ d_{j+1}^1[n_1, n_2] &= a_j[n_1, n_2] * h_d[2n_1] g_d[2n_2] \\ d_{j+1}^2[n_1, n_2] &= a_j[n_1, n_2] * g_d[2n_1] h_d[2n_2] \\ d_{j+1}^3[n_1, n_2] &= a_j[n_1, n_2] * g_d[2n_1] g_d[2n_2]. \end{aligned} \quad (6)$$

The convolution equations form 6 are computed with only six groups of one dimensional convolutions. The rows of a_j are first convolved with h_d and g_d and subsampled by 2. Then, the columns of these two output images are convolved with h_d and g_d and subsampled, resulting four subsampled images a_{j+1} , d_{j+1}^1 , d_{j+1}^2 and d_{j+1}^3 . Figure2 illustrates one level 2D DWT decomposition.

Similar to classical DWT, 2D DWT is a non-redundant transform, the wavelet image representation of x , at resolution J :

$$\left[a_j, \{d_j^1, d_j^2, d_j^3\}_{0 < j \leq J} \right]$$

having the same size as the original two-dimensional signal, x . In the coefficients image, the coefficients' repartition is presented in Figure 2.11, where 'LL' (a) are the approximation coefficients, 'LH' (d^1) the horizontal details, 'HL' (d^2) the vertical details and 'HH' (d^3) the diagonal details. A second order statistical analysis of 2D DWT is presented in [7].

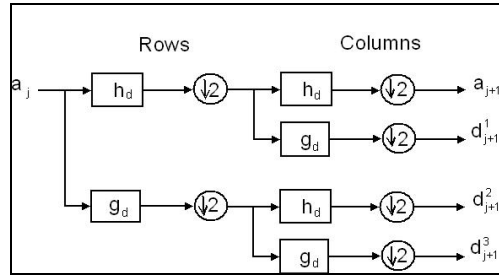


Figure 2. One-level 2D DWT Decomposition Scheme

LL (a)	HL (d ²)
LH (d ¹)	HH (d ³)

Figure 3. 2D DWT Coefficients' Image

In what concerns the reconstruction part, the 2D DWT, same as the DWT, ensures perfect reconstruction if the conditions given by theorem of Vetterli [8] are fulfilled. The reconstruction formula for the approximation coefficients at level j , a_j from the coarser scale approximations a_{j+1} and the wavelet coefficients d_{j+1}^k , $1 \leq k \leq 3$ is:

$$a_j[n_1, n_2] = \check{a}_{j+1}[n_1, n_2] * h[n_1]h[n_2] + \check{d}_{j+1}^1[n_1, n_2] * h[n_1]g[n_2] + \check{d}_{j+1}^2[n_1, n_2] * g[n_1]h[n_2] + \check{d}_{j+1}^3[n_1, n_2] * g[n_1]g[n_2]$$

Where, with $\check{x}[n_1; n_2]$ we have denoted the image twice the size of $x[n_1, n_2]$, obtained by inserting a row of zeros and a column of zeros between pairs of consecutive rows and columns.[8]

The corresponding implementation scheme is presented in Figure 4.

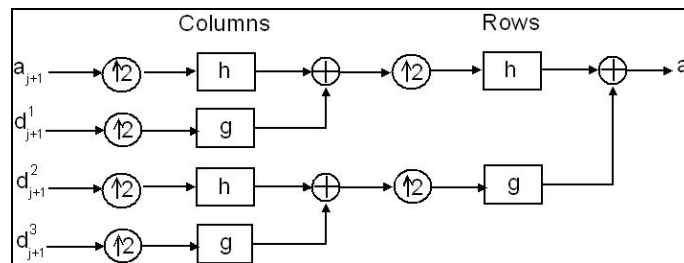


Figure 4. One-level 2D DWT Reconstruction Scheme

4. The Translation Invariant Wavelet Representations

In this section, we describe an alternative wavelet representation, which is an extension to the standard wavelet decomposition. It is invariant to translations in the sense that it looks at all the translates of the input image and chooses the best set of wavelet coefficients. It consists of two key steps: an efficient algorithm for computing the wavelet transforms for all the translates and a fast quadtree search algorithm.

4.1. Computing the Wavelet Transforms for all the Translates

Beylkin described an $O(N \log N)$ algorithm to obtain the wavelet transforms for all the circular shifts of a onedimensional signal in [9]. Our method described here is an extension of this algorithm to the two dimensionial case.

We know that the wavelet transform of a $N \times N$ image takes $O(N^2)$ operations. To compute the wavelet transforms for all the N^2 translates of the image seems to take $O(N^4)$ operations. However, due to the periodicity of the rate change operators in the decomposition subbands, the computational load can be greatly reduced to $O(N^2 \log N)$.

First, let us look at what happens at the initial decomposition stage: the image is divided into 4 channels; then, the four subimages are downsampled by a factor of two both by column and by row. The rate-change operator divides the image into 4 cosets. Given any translation of the input, the output subimages can be obtained by simply circularly shifting one of these four cosets. Therefore, it is sufficient to calculate the outputs for only four different translates representing the four different cosets, and the output of any circular shift of the input can be reproduced from one of these 4 sets. Note that the four cosets correspond to the outputs for the translates: (0,0), (0,1), (1,0), (1,1) respectively.

By the same token, we need only to keep the outputs of four translates at the second stages for each of the four inputs from the first stage. At the second stage, the size of the image is halved (one fourth the number of coefficients) and the number of subimages quadruples, making the total number of coefficients constant, namely $3N^2$. We may repeat this procedure, and a complete decomposition tree (Figure.5) will have $N^2(3 \log N + 1)$ elements.

On each scale j , ($1 \leq j \leq \log N$), we compute 4^j vectors of averages and 4^j vectors of differences.

Let $A_{2^{j+1}}(k,s)$, $k, s = 1, 2, 3, \dots, 2^{\log N - j + 1}$ be one of the vectors of averages at the previous scale $j+1$, we compute 4 average outputs.

$$A_{2^j}^{(0,0)} = \sum_{(m,n)} h(n)h(m)A_{2^{j+1}}(n + 2k, m + 2s) \quad (7)$$

$$A_{2^j}^{(0,1)} = \sum_{(m,n)} h(n)h(m)A_{2^{j+1}}(n + 2k, m + 2s + 1) \quad (8)$$

$$A_{2^j}^{(1,0)} = \sum_{(m,n)} h(n)h(m)A_{2^{j+1}}(n + 2k + 1, m + 2s) \quad (9)$$

$$A_{2^j}^{(1,1)} = \sum_{(m,n)} h(n)h(m)A_{2^{j+1}}(n + 2k + 1, m + 2s + 1) \quad (10)$$

The two-dimensional periodic sequence $A_{2^j}^{(0,0)}$ contains all the coefficients that appear if $A_{2^{j+1}}$ is shifted by (0, 0), (2,2), (4,4),....The similar statements are true for $A_{2^j}^{(0,1)}$, $A_{2^j}^{(1,0)}$, $A_{2^j}^{(1,1)}$. In the same manner, the differences for all the different translates can be obtained by just computing the differences for 4 shifts. Repeating this procedure recursively, we can get the wavelet coefficients for all translates in $\log N$ steps with $O(N^2 \log N)$ operations. The decomposition procedure leads naturally to a quadtree structure as in Figure5.

While the quadtree decomposition contains all the coefficients we need to form the wavelet transform for any translate, these coefficients are not organized sequentially, and therefore must be addressed in a proper manner. Suppose we want the wavelet transform for the translate (m, n):

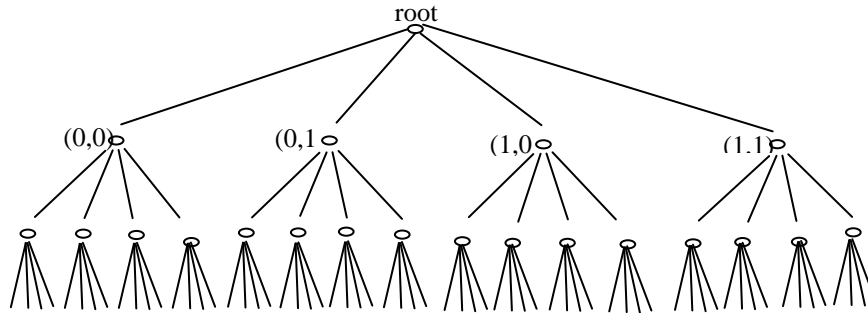


Figure 5. The Decomposition Tree Contains i information to Form the Wavelet Transforms of all the Circular Translates. Each Node Stands for the Three sub-Band Images at a Given Scale. The Four Children of each Node Correspond to the Four Cosets

4.2. Search for the Minimal Cost Coefficients

We start from the leaves and work bottom-up for the four child nodes of the same parent, we choose the one with the minimal cost, and repeat the operation recursively. The additivity of the cost function enables us to complete the search in $O(N^2 \log N)$ operations.

Many additive cost functions exist. The Mean Squared Error is the most popular one. Other additive cost functions, such as vector entropy and threshold counting, have also been used. Lately, the work by Ramchandran and al [10] proposes to use the Rate-Distortion (R-D) criterion. The choice of the cost function affects the wavelet representation resulted, and should be chosen with care. In data compression applications, the cost function should be related to either the bit-rate or the distortion. In multiresolution detection, the cost function may be related to the detection probability or the false-alarm rate [11].

5. Experiment Results

For learning, a species of ultrasound images 292x400 pixels is used. We load our image and resize it where ($N=256$) is the number of pixels which consist of two different grey level values, and we add White Gaussian Noise with different values of sigma to obtain denoised one as shown in Figure 6.

Then we compute the orthogonal 2D wavelet transform for the noised one and we reconstruct it as shown in Figure 7.

Another way to achieve translation invariance is to replace the orthogonal 2D wavelet by a redundant translation invariant wavelet. First we compute the translation invariant wavelet transform, We can now reconstruct our image.

We try to compare the results obtained using a nonlinear filter such as wiener filter 2D applied to a noisy and binary image. The results are shown in the Figure 8 below:

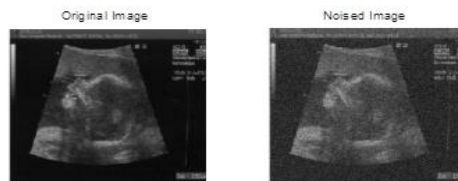


Figure 6: Original Image and its Noised One

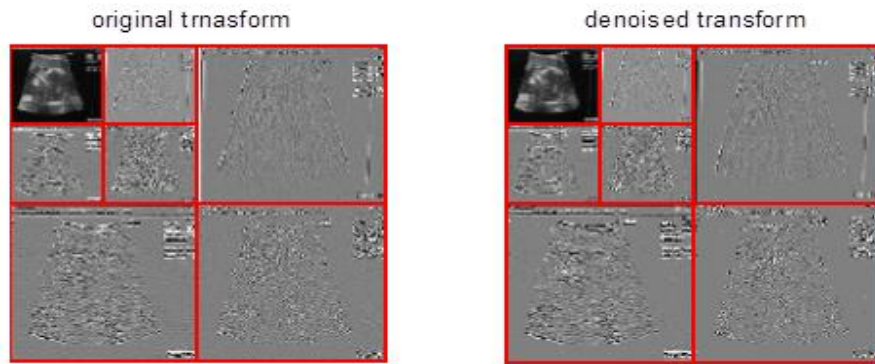


Figure 7. Orthogonal 2D Wavelet Transform for the Noised One and its Denoised One

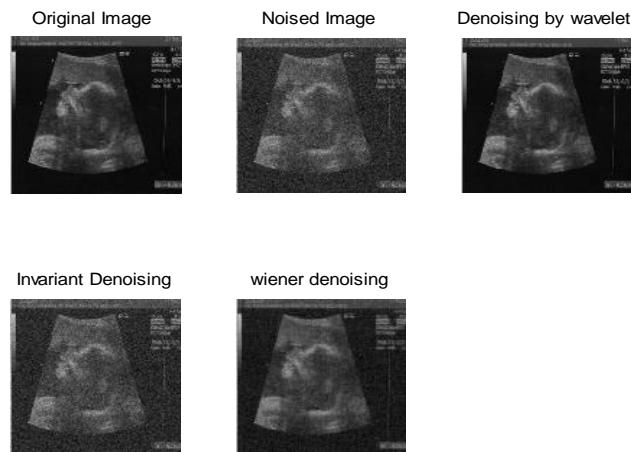


Figure 8. Original Image(a), Noised Image(b), Denoising by Wavelet(c), Invariant Denoising(d), Wiener Denoising(e)

To measure the quality between the original image and the filtered, another comparison is performed by calculating the PSNR calculates the peak signal- to- noise ratio between two images. The higher PSNR means the quality of the image treated is better. The PSNR is calculated using the following equation:

$$PSNR = 10\log_{10}\left(\frac{R^2}{MSE}\right) \quad (11)$$

In the above equation, R is the maximum variation in the data type of the input image. For example, if the input image is double, then R is 1. If it is of unit 8, R is 255. MSE is the mean square error (MSE) which is the square of the accumulated error between the original and filtered image. The lower value of MSE means the error is small. MSE is calculated using the following equation:

$$MSE = \frac{\sum_{M,N}[I_1(m,n) - I_2(m,n)]^2}{M \cdot N} \quad (12)$$

In the above equation, M and N are the number of rows and columns in the input images, respectively.

The mean square error (MSE) and peak ratio of signal to noise (PSNR) are the two error parameters used to compare the quality of image compression.

The comparison results are shown in the following table:

Tableau 1. Comparison between original image(a), noised Image(b), denoising by wavelet(c), Invariant Denoising(d), wiener denoising(e) for sigma=0.06.

ImagesSigma=0.06	PSNR T=0.01	PSNR T=0.1	PSNR T=0.5	PSNR T=1
(a,b)	27.1022	26.6994	26.8761	27.1519
(b,c)	27.0857	26.0718	24.7121	17.5050
(b,d)	61.3600	29.8321	25.6324	17.8027
(b,e)	29.0368	28.6649	28.8526	29.1402

Tableau 2. Comparison between Original Image(a), Noised Image(b), Denoising by Wavelet(c), Invariant Denoising(d), Wiener Denoising(e) for Sigma=0.08

Images Sigma=0.08	PSNR T=0.01	PSNR T=0.1	PSNR T=0.5	PSNR T=1
(a,b)	24.7846	24.5701	24.9866	24.8231
(b,c)	24.7735	24.2088	23.6499	17.3312
(b,d)	62.7815	30.7952	24.4244	17.6818
(b,e)	29.2147	28.9968	29.3056	29.2302

Tableau 3. Comparison between Original Image(a), Noised Image(b), Denoising by Wavelet(c), Invariant Denoising(d), Wiener Denoising(e) for Sigma=0.1

Images Sigma=0.1	PSNR T=0.01	PSNR T=0.1	PSNR T=0.5	PSNR T=1
(a,b)	22.8787	23.0136	23.5682	23.0843
(b,c)	22.8717	22.7729	22.6378	17.1116
(b,d)	63.7546	32.1282	23.3586	17.5031
(b,e)	29.5341	29.6286	30.2330	29.7066

Tableau 4. Comparison between Original Image(a), Noised Image(b), Denoising by Wavelet(c), Invariant Denoising(d), Wiener Denoising(e) for Sigma=0.5

Images Sigma=0.5	PSNR T=0.01	PNR T=0.1	PSNR T=0.5	PSNR T=1
(a,b)	14.5607	14.7825	15.0051	14.4493
(b,c)	14.5608	14.7705	14.9626	13.9776
(b,d)	76.1212	46.3478	23.9382	15.7536
(b,e)	42.7010	42.9635	43.3301	42.7123

Tableau 5. Comparison between Original Image(a), Noised Image(b), Denoising by Wavelet(c), Invariant Denoising(d), Wiener denoising(e) for Sigma=5

Images Sigma=5	PSNR T=0.01	PSNR T=0.1	PSNR T=0.5	PSNR T=1
(a,b)	12.5061	13.3000	13.0070	13.0781
(b,c)	12.5060	13.3000	13.0061	13.0729
(b,d)	104.0839	74.8734	53.6177	44.5610
(b,e)	77.5280	78.1473	78.0564	77.8293

Tableau 6. Comparison between Original Image(a), Noised Image(b), Denoising by Wavelet(c), Invariant Denoising(d), Wiener denoising(e) for Sigma=30

Images Sigma=30	PSNR T=0.01	PSNR T=0.1	PSNR T=0.5	PSNR T=1
(a,b)	12.1704	12.0935	12.1451	12.4132
(b,c)	12.1704	12.0936	12.1451	12.4129
(b,d)	127.2698	97.4059	75.8513	67.1946
(b,e)	107.2776	107.3828	103.6860	105.3771

After the comparison between the results obtained when we have used different values of sigma, It is clear that the value of PSNR is high in the case of the comparison between (noised Image (b) and Invariant Denoising(d)) where T=0.01 which means that image quality is better using the technique of invariant translation denoising than a filter Median to eliminate noise in medical imaging.

6. Conclusion

We have discussed in this paper the use of wavelets especially invariant translation wavelet 2D in reducing noise which has a bad effect on medical imaging thus the degradation of its quality.

This manuscript is organized in five sections. Section 1 presents an introduction of the medical imaging and the methods used in reducing the noise. Section 2 describes the basics of wavelets when used as filter. The two dimensional dwt is studied in Section 3 and the translation invariant wavelet representations in Section 4. In Section 5 we have applied the dwt2d and translation invariant wavelet on the medical image and were completed by comparing the results obtained with those obtained by median filter. Section 6 draws the conclusion of this study.

In this paper we have demonstrated that the use of translation invariant wavelet could offer better results than those obtained by the commonly used median filter. It still needs a clinical trial and verification to demonstrate the additional benefit.

The main message of this study is to validate this strategy in a simple and a controlled experimental environment.

References

- [1] X. Zong, A. F. Laine and E. A. Geiser, "Speckle Reduction and Contrast Enhancement Of Echocardiograms Via Multiscale Nonlinear Processing", IEEE Trans On Median Imaging, vol. 17, (1998).
- [2] E. P. Simonelli and E. H. Adelson, "Noise Removal Via Bayesian Wavelet Coring", Proc. 3rd Int. Conf On Image Processing, vol. 1, (1996).
- [3] A. Achim, A. Bezerianos and P. Tsakalides, "Ultrasound Image Denoising Via Maximum A Posteriori Estimation Of Wavelet Coefficients", Proc. IEEE EMBS 23rd Annual Int. Conf., vol. 3, (2001).
- [4] M. Karaman, M. A. Kutay and G. Bozdagi, "An Adaptive Speckle Suppression Filter For Medical Ultrasonic Imaging", IEEE Trans. Medical Imaging, (1995), vol. 14, no. 2.
- [5] Y. Yu and S. T. Acton, "Speckle Reducing Anisotropic Diffusion", IEEE Transactions On Image Processing, vol. 11, no. 11, (2002) November.
- [6] C.-Lin, "Discrete Wavelet Transform: A Tutorial of the Wavelet Transform", Liu, (2010) February 23.
- [7] C. Nafornita, I. Firoiu, D. Isar, J.-M. Boucher and A. Isar, "A Second Order Statistical Analysis of the 2d Discrete Wavelet Transform", Proceedings of International Conference Communications, Bucharest, (2010).
- [8] I. Adam, "Complex Wavelet Transform: Application to Denoising", Phd Thesis, The Politehnica University Of Timisoara And Université De Rennes 1, (2010).
- [9] G. Beylkin, "On the Representation Of Operators In Bases Of Compactly Supported Waveltes", Siam J. Numer. Anal, vol. 29, no. 6, (1992), pp. 1716-1740.

- [10] K. Ramachandran and M. Vetterli, "Best Wavelet Packet Bases In A Rate-Distortion Sense", IEEE Tra 2. Image Processing, (1993) April, pp. 160-175.
- [11] J. Liang Thomas W, Parks, "A Two-Dimensional Translation Invariant Wavelet Representation And Its Applications", IEEE, (1994).

Author

R. Bouchouareb, received the Engineering studies from the Department of electrical engineering, BATNA University, ALGERIA in 2002. The Master degree in Telecommunication from Department of Electrical Engineering, BATNA University, ALGERIA, in 2010. Currently, she is a student Ph.D. in Electrical Engineering, BATNA University, ALGERIA. rachidabouchouareb@gmail.com.